water

MDPI

*Article*

# Lanthanum and Sludge Extracellular Polymeric Substances Coprecipitation-Modified Ceramic for Treating Low Phosphorus-Bearing Wastewater

**Yao-Yao Lu, Chao-Xi Yang, Ke-Yu Chen, Jiao-Jiao Wang *, Bao-Cheng Huang and Ren-Cun Jin**

School of Engineering, Hangzhou Normal University, Hangzhou 310018, China; luyaoyao1@stu.hznu.edu.cn (Y.-Y.L.); yangchaoxi@stu.hznu.edu.cn (C.-X.Y.); chenkeyu@stu.hznu.edu.cn (K.-Y.C.); huangbc@hznu.edu.cn (B.-C.H.); rcjin@hznu.edu.cn (R.-C.J.)

* Correspondence: 20127004@hznu.edu.cn

**Abstract:** Excessive phosphorus discharge from fertilizers and detergents has caused severe eutrophication in water bodies, necessitating the upgrading of efficient and cost-effective adsorbents for phosphorus removal. In this study, a novel lanthanum and extracellular polymeric substance (EPS) coprecipitation-modified ceramic (La-EPS-C-450) was developed to address the limitations of existing adsorbents. The ceramic filler served as a robust and scalable matrix for lanthanum loading, while EPS introduced functional groups and carbonate components that enhanced adsorption efficiency. The prepared adsorbent manifested a maximum phosphorus adsorption capacity of 83.5 mg P/g-La at 25 °C, with its performance well expressed by the Freundlich isotherm model, indicating that it was a multilayer adsorption process. The adsorption mechanism was driven by electrostatic attraction and ligand exchange between lanthanum and phosphate ions, forming inner-sphere complexes. The material demonstrated unfluctuating performance across a pH range of 3–7 and retained high selectivity in the presence of competing anions. In practical applications, La-EPS-C-450 effectively removed phosphorus from actual river water, achieving a treatment capacity of 1800 bed volumes in a continuous-flow fixed column system. This work provides valuable insights into the progress of advanced ceramic-based adsorbents and demonstrates the potential of La-EPS-C-450 as a cost-efficient and effective material for phosphorus removal in water treatment applications.

**Keywords:** phosphorus removal; adsorbent; lanthanum; ceramic; extracellular polymeric substances

check for updates

Academic Editor: Constantinos V. Chrysikopoulos

Received: 28 March 2025
Revised: 19 April 2025
Accepted: 19 April 2025
Published: 21 April 2025

**Citation:** Lu, Y.-Y.; Yang, C.-X.; Chen, K.-Y.; Wang, J.-J.; Huang, B.-C.; Jin, R.-C. Lanthanum and Sludge Extracellular Polymeric Substances Coprecipitation-Modified Ceramic for Treating Low Phosphorus-Bearing Wastewater. *Water* **2025**, *17*, 1237. https://doi.org/10.3390/w17081237

**Copyright:** © 2025 by the authors. Licensee MDPI, Basel, Switzerland. This article is an open access article distributed under the terms and conditions of the Creative Commons Attribution (CC BY) license (https://creativecommons.org/licenses/by/4.0/).

## 1. Introduction

Excessive use of chemical fertilizers and detergents has resulted in the discharge of phosphorus-containing compounds into water bodies, leading to the eutrophication and disruption of ecological stability. Removing excessive phosphorus from water is therefore essential for mitigating eutrophication in surface waters [1,2]. Among the available methods, adsorption has proven to be an effective approach to treating phosphorus-contaminated water owing to its facility, efficiency, and adaptability [3]. The performance of adsorption depends heavily on the characteristics of the adsorbent and the conditions under which the adsorption process occurs. An ideal adsorbent should exhibit key attributes such as high adsorption capacity, rapid adsorption rate, excellent selectivity, long-term stability, and minimal environmental impact [4].

Metal oxide and hydroxides, such as those incorporating aluminum, iron, calcium, magnesium, lanthanum, and cerium, are commonly used as adsorbents due to their high

affinity for phosphate [5]. Among these, lanthanum-based materials are particularly noteworthy owing to their superior phosphate adsorption capacity [6]. However, the practical application of nanoscale lanthanum-based adsorbents is constrained by challenges associated with their separation from treated water and the high costs involved. Consequently, research efforts have increasingly focused on developing composite adsorbents that address these limitations and are suitable for practical, large-scale applications [7–9]. To achieve effective immobilization of lanthanum ions ($La^{3+}$) onto carrier matrices, contemporary advanced materials—including interlayer materials and lanthanum-based nanocomposites—primarily rely on ligand exchange or interlayer intercalation mechanisms to incorporate $La^{3+}$ into the carrier structure. Extensive studies have confirmed that functional groups such as carboxyl (-COOH) and hydroxyl (-OH) exhibit robust cross-linking interactions with multivalent metal ions [10–12]. Notably, Fu and Kong demonstrated the successful immobilization of $La^{3+}$ on a carrier matrix through a coprecipitation-assisted cross-linking approach, capitalizing on these synergistic interactions [13,14].

Ceramic materials have attracted attention as promising adsorption carriers due to their widespread availability, cheapness, and structural robustness. The adsorption performance of ceramics is closely connected with their surface functional group content, which can be tuned by varying the precursor composition and preparation conditions [15]. Sludge extracellular polymeric substances (EPSs), which are composed of proteins and polysaccharides, contain functional groups such as carboxyl and hydroxyl which can interact with some metal through ion exchange, electrostatic attraction, surface precipitation, or other mechanisms [16,17]. Additionally, the carbon-rich components of EPSs can undergo pyrolysis to form biochar-like structures, which further enhance their ability to adsorb phosphorus [18,19]. Herein, by modifying ceramic with EPSs, lanthanum ions can potentially be immobilized onto the ceramic surface through precipitation, yielding an efficient phosphorus adsorbent.

In this work, an original lanthanum-modified ceramic adsorbent was developed with the goal of enhancing phosphorus removal efficiency. Commercially available ceramics were utilized as the base material, and a combination of surface precipitation and calcination treatments was applied to immobilize lanthanum onto the ceramic matrix. The physicochemical properties of the modified ceramics were comprehensively characterized, and their phosphorus removal performance was evaluated and the adsorption mechanism was discussed. Additionally, the long-term performance of our modified ceramic under continuous flow conditions was investigated and compared to the commercial lanthanum-modified bentonite (LMB) material. The results of this research provide valuable insights into the development of low-cost and efficient adsorbents for phosphorus removal from aquatic systems.

## 2. Materials and Methods

### *2.1. Chemicals and Materials*

Ceramic materials were purchased from Gongyi Youlan Co., Ltd. (Gongyi, China), with porosity and specific gravity of 40% and 1.06 $g/cm^3$, respectively. LMB (Phoslock®) was purchased from Phoslock Environmental Technologies Co., Ltd. (Shanghai, China). Detailed information on the chemical reagents used is provided in Section S1.

### *2.2. Adsorbent Preparation*

Sludge EPS was extracted via a thermal extraction method [20] and its content was quantified by a total organic carbon analyzer (TOC-L, Shimadzu, Kyoto, Japan). A detailed extraction procedure was provided in Section S2.

The modified ceramic adsorbent was prepared through a multi-step process. Initially, the raw ceramic material was cleaned with deionized water to wash ash and impurities and then dried in an oven at 105 °C for 24 h. The dried ceramic (5 g) was immersed in 100 mL of EPS solution with a TOC content of 0.80 g/L. This step was conducted for 9 h to ensure thorough interaction between the ceramic surface and EPS. Subsequently, 50 mL of lanthanum chloride solution (0.4 M) was added to the EPS-treated ceramic under continuous stirring, facilitating the precipitation of lanthanum onto the surface of the ceramic via EPS flocculation. After reaction for another 9 h, the modified ceramics were collected and dried at 105 °C for 24 h and then calcined in a tube furnace under a $N_2$ atmosphere at 450 °C for 2 h. The resultant material was designated as La-EPS-C-450. For comparison, under the same preparation conditions, a ceramic modified only with lanthanum (without EPS) was prepared and denoted as La-C-450. A more detailed method is supplemented in Section S3.

### *2.3. Characterization of Adsorbent*

The surface morphology and element distribution of the material were characterized by field emission scanning electron microscopy (SEM, ZEISS Sigma 300, Oberkochen, Germany) equipped with an energy dispersive spectrometer (EDS). The elemental composition of La-EPS-C-450 was examined by X-ray photoelectron spectroscopy (XPS, AXIS Ultra, Shimazdu, Japan). The surface pore characteristics distribution was determined using $N_2$ adsorption–desorption isotherms (Autosorb-IQ3, Quantachrome, Beijing, China). The lanthanum content loaded onto the ceramic and leakage was measured by inductively coupled plasma emission spectroscopy (ICP-OES). Fourier-transformed infrared spectroscopy (FTIR Nicolot 5700, Thermo Fisher Scientific, Shanghai, China ) was employed to analyze surface functional groups.

### *2.4. Batch-Scale Adsorption Experiment and Kinetic Analysis*

In a typical adsorption experiment (100 mL), 5 g of adsorbent was added into a phosphorus stock solution (20 mg/L, pH = 6.7 ± 0.2) at 25 °C. The phosphorus adsorption thermodynamics were also evaluated by changing the adsorption temperature to 15 °C and 35 °C, respectively. The adsorption kinetics were analyzed using pseudo-first-order and pseudo-second-order kinetic models, while adsorption isotherms were evaluated using the Langmuir and Freundlich isotherm equations.

$$ln(Qe - Qt) = lnQe - lnk_1 t \quad (1)$$

$$\frac{t}{Qt} = \frac{1}{k_2 Qe_2} + \frac{1}{Qe}t \quad (2)$$

$$Qt = \frac{(C0 - Ct)v}{m} \quad (3)$$

$$Qe = \frac{QmkLCe}{1 + kLCe} \quad (4)$$

$$Qe = kFCe^{\frac{1}{n}} \quad (5)$$

$Q_e$ (mg/g) is the saturated adsorption capacity, $Q_t$ (mg/g) is the adsorption capacity in a definite time $t$, $k$ is the kinetic constant, $C_0$ (mg/L) is the initial phosphorus concentration, $C_t$ (mg/L) is the phosphorus concentration at reaction time $t$, $Q_m$ (mg/g) is the maximum adsorption capacity, and $C_e$ (mg/L) is the phosphate concentration at equilibrium.

### *2.5. Continuous-Flow Adsorption Column Test*

To acquire the application potential of the lanthanum-modified ceramic for treating phosphorus in real water bodies, a continuous-flow adsorption column experiment was performed. An up-flow column with a total volume of 60 mL was used and the adsorbents were packed into a column with a volume ratio of 30%. Surface water collected from the local Yuhangtang River (Hangzhou, China) was fed into columns. The influent rate was maintained at 10 mL/min, and the test was conducted at ambient temperature (18 ± 7 °C).

## 3. Results and Discussion

### *3.1. Synthesis and Structural Characterization of Adsorbent*

Figure 1 illustrates the morphology of ceramic, La-C-450 and La-EPS-C-450. Compared with the smooth surface of the unmodified ceramic, La-EPS-C-450 exhibits more distinct block-like structures on its surface, indicating an improved dispersion of lanthanum. EDS (Figure 1d) confirmed the loading of lanthanum on the ceramic surface. The escape of EPS-rich organic matter during pyrolysis likely promoted the formation of these block-like structures. The $N_2$ adsorption–desorption isotherm of La-EPS-C-450 (Figure 1e,f) displayed a type IV curve with an H3 mesoporous hysteresis loop, indicating a rich slit-type mesoporous structure. The pore size of the material spans both mesopores and macropores, which provides favorable conditions for the dispersion of lanthanum. Compared with the concentrated pore distribution of La-C-450, the increase in the proportion of mesopores and micropores of La-EPS-C-450 may mean that the metal lanthanum is well dispersed [21].

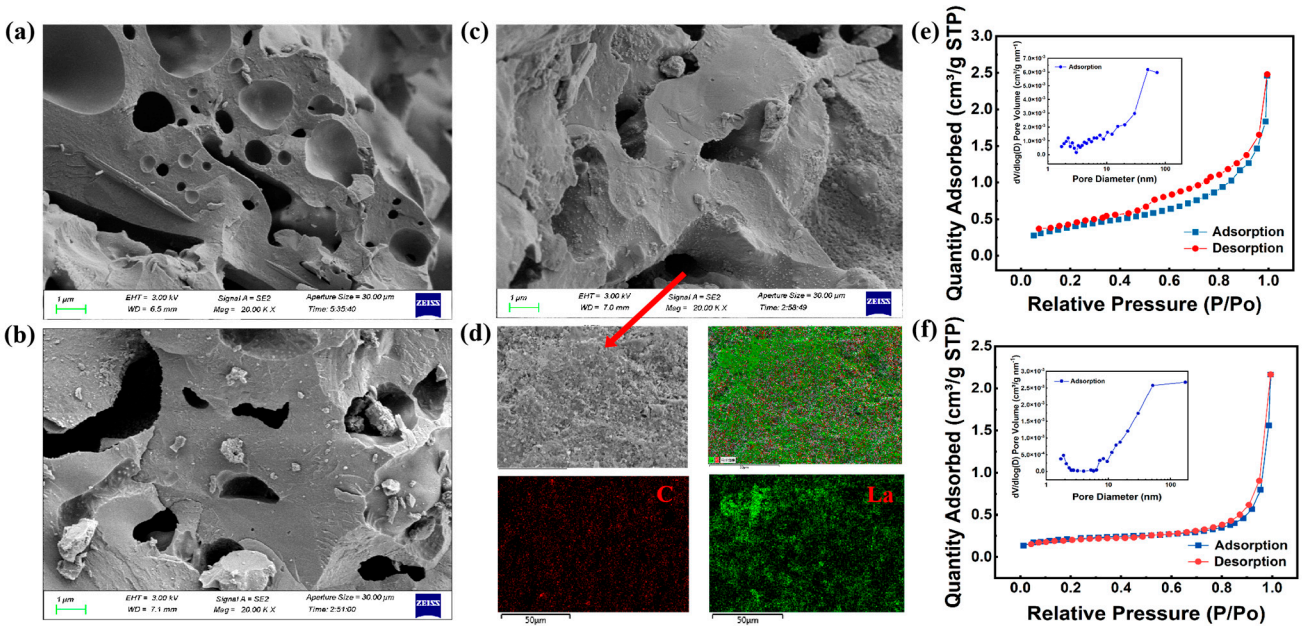



**Figure 1.** Surface morphology characterizations. SEM images of raw ceramic (**a**), La-C-450 (**b**) and La-EPS-C-450 (**c**), EDS of La-EPS-C-450 (**d**), and $N_2$ adsorption isotherms and pore size distribution curves of La-C-450 (**e**) and La-EPS-C-450 (**f**).

### *3.2. Adsorption Kinetics and Thermodynamics*

To investigate the phosphorus removal characteristics of the modified ceramics, adsorption experiment kinetic data were analyzed by pseudo-first-order kinetic model and pseudo-second-order kinetic model. Among the materials tested, La-EPS-C exhibited the fastest adsorption rate and the highest adsorption capacity at a carbonization temperature of 450 °C (Figure 2a). The maximum phosphorus adsorption capacity, determined through

kinetic model fitting, was 83.51 mg P/g-La. Adsorption equilibrium was achieved within 7 h, after which the adsorption curve plateaued (Figure 2b).

The isotherm models were applied to fit the adsorption data (Figure 2c), and the relevant parameters are presented in Table 1. The Langmuir isothermal adsorption model, which describes monolayer chemical adsorption, indicated a fitting highest phosphorus adsorption capacity of 74.42 mg P/g-La at 35 °C, which is higher than the other reported composite adsorbents (Table 2). Thermodynamic analysis showed that phosphorus adsorption capacity increased with temperature. The Freundlich model, better fitting the adsorption process at varying temperatures, suggested that adsorption occurred on heterogeneous surface sites, involving multilayer adsorption. This observation was attributed to the complex pore structure of La-EPS-C-450. The Freundlich parameter 1/n values were less than 0.48 at 15 °C and 35 °C, indicating synergistic adsorption effects at these temperatures. At 25 °C, 1/n exceeded 0.48, highlighting a shift in adsorption behavior [22,23].

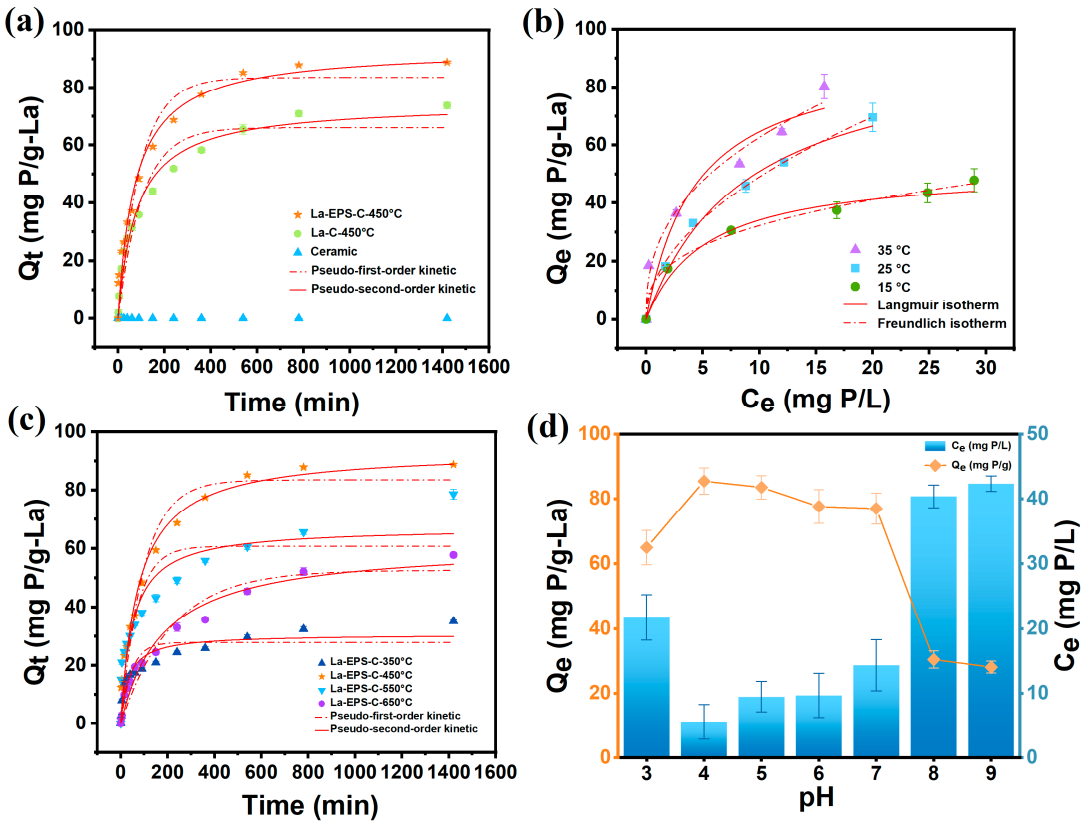



**Figure 2.** Phosphorus adsorption characteristic by the as-prepared materials. Kinetic model fitting results of the as-prepared adsorbents (**a**,**b**), Langmuir and Freundlich fitting equations for phosphate adsorption by La-EPS-C-450 (**c**), effects of pH on the adsorption capacity of La-EPS-C-450 (**d**).

**Table 1.** Langmuir and Freundlich fitting parameters for phosphate adsorption by La-EPS-C-450.

| Adsorbent | Temperature | Langmuir | | | Freundlich | | |
|---|---|---|---|---|---|---|---|
| | | $R_1^2$ | Qmax (mg/g-La) | $K_L$ (L/mg) | $R_2^2$ | $K_f$ (mg/g-La) | 1/n |
| La-EPS-C-450 | 35 °C | 0.86 | 74.42 | 0.23 | 0.98 | 25.23 | 0.39 |
| La-EPS-C-450 | 25 °C | 0.98 | 69.33 | 0.11 | 0.99 | 15.12 | 0.51 |
| La-EPS-C-450 | 15 °C | 0.95 | 45.82 | 0.19 | 0.99 | 14.37 | 0.35 |

The adsorption performance of La-EPS-C-450 was influenced by solution pH, as pH affects the charge of the adsorbent surface and chemical speciation of phosphate ions in water. Neutral and acidic environments are more conducive to the adsorption of the

La-EPS-C-450. At high pH values, the adsorbent surface carries more negative charges, leading to electrostatic repulsion with negatively charged phosphate species [24]. When the pH is below 6, the surface of the adsorbent is protonated to form positively charged species (La-$OH^{2+}$) which interact with phosphate ions according to the electrostatic attraction [25]. Changes in the isoelectric point (IEP), potentially owing to the formation of inner-sphere complexes (Figure S2), suggest that the adsorption mechanism involves both electrostatic attraction and the formation of inner- and outer-sphere complexes [26]. Phosphate speciation also varies with pH changes. In the pH range of 2–4, $H_3PO_4$ transforms to $H_2PO_4^-$ [27], allowing adsorption to occur predominantly via electrostatic interactions. At pH 5–7, both $H_2PO_4^-$and $HPO_4^{2-}$ are present, with the formation of $LaPO_4$ complexes gradually becoming significant [28]. At higher pH levels, the predominance of $HPO_4^{2-}$ species reduces adsorption efficiency, as $HPO_4^{2-}$ behaves with more powerful adsorption free energy but is less readily captured by the adsorbent [29]. Consequently, adsorption capacity decreases at elevated pH levels (Figure 2d).

### *3.3. Adsorption Mechanism*

The FT-IR spectra revealed significant alterations in the material before and after phosphate adsorption. The peak at 1053 $cm^{-1}$ (Figure 3a) resembles the P-O asymmetric stretching vibration of $PO_4^{3-}$, while peaks at 619 $cm^{-1}$ and 543 $cm^{-1}$ correspond to the bending vibration of the O-P-O group [30,31]. These peaks were observed after phosphate adsorption, confirming phosphate was adsorbed to the material successfully. Additionally, the La-O vibration frequency shifted from 541 $cm^{-1}$ to 543 $cm^{-1}$ after phosphate adsorption (Figure 3a), further supporting this observation. A weakening of the antisymmetric stretching vibration peak of $CO_3^{2-}$ around 1429/1490 $cm^{-1}$ (Figure 3b) suggests an in situ substitution reaction between $CO_3^{2-}$ and $H_2PO_4^-$ or $HPO_4^{2-}$. The wide band at 3500 $cm^{-1}$, corresponding to the stretching and bending vibration of –OH groups [32], also weakened after phosphate adsorption. This could be due to the decrease in $La(OH)_3$ content or substitution of hydroxyl groups by the La-O-P surface complex [33]. The comodification of lanthanum and EPS enhanced the resonance vibrations of hydroxyl and carbonate groups, which were subsequently weakened after phosphate adsorption. These results suggest that ligand exchange among -OH, $CO_3^{2-}$, and $PO_4^{3-}$ dominated the adsorption process.

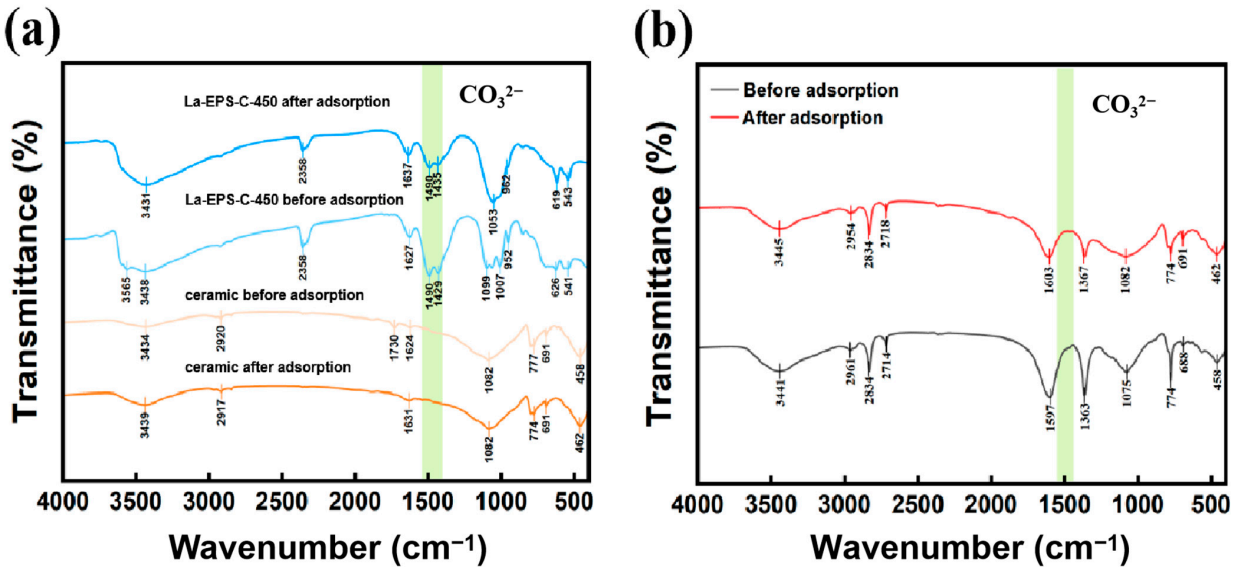



**Figure 3.** Adsorbent surface functional group variations before and after phosphorus adsorption. FT-IR spectra of raw ceramic and La-EPS-C-450 (**a**) and La-C-450 (**b**).

XPS analysis of La 3d before (Figure 4a) and after (Figure 4b) phosphate adsorption showed a shift in binding energy. The La $3d_{5/2}$ double peaks shifted to 835.30 and 838.50 eV, and La $3d_{3/2}$ peaks shifted to 852.10 and 855.70 eV. This 0.2–0.8 eV shift indicates valence band electron transfer and the formation of inner-sphere recombination between La and P [34,35]. This phenomenon aligns with the La-O-P complex formation observed in FT-IR spectra at 543 $cm^{-1}$ [25]. After phosphate absorption, the peak intensity of O-C=O peak in FT-IR spectra decreased. This indicates that when phosphate is adsorbed onto La-EPS-C-450, the ligand exchange between phosphate in water and the carbonate group of La-EPS-C-450 occurs [36]. By the peak quantification of the XPS of the carbon atom, a distinct peak near a binding energy of 289 eV was observed (Figure 4e), corresponding to carbonate functional groups. The higher content of carbon carbonate atoms compared to the raw ceramic and La-C-450 suggests that lanthanum may have formed lanthanum carbonate on the ceramic (Figure 4f), which is likely the main active component for phosphorus adsorption [37]. The baseline before adsorption and the significant phosphorus peak after adsorption also indicated that phosphorus was successfully adsorbed (Figure 4d).

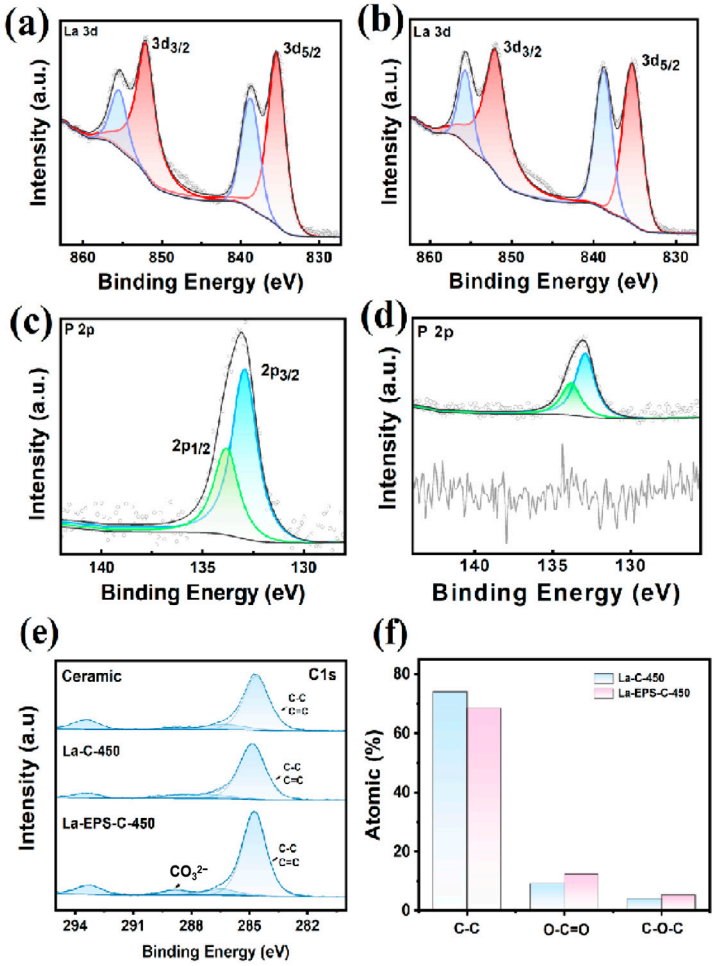



**Figure 4.** XPS survey of materials. La 3d of La-EPS-C-450 before (**a**) and after (**b**) adsorption, P 2p patterns of La-EPS-C-450 before (**c**) and after (**d**) adsorption, C 1s patterns (**e**) and the relative percentages (**f**) of different materials before adsorption.

### *3.4. Practical Application Potential of the Adsorbent*

In real-world applications, the adsorption of phosphate was affected by the coexisting anions in water. Outer-sphere complexes, which rely on electrostatic interactions, are highly sensitive to competitive anions. Conversely, inner-sphere complexes, formed by bonding with surface groups directly, are largely unaffected by coexisting anions [25,38].

Our experiments demonstrated that common anions such as $Cl^-$, $NO_3^-$, $SO_4^{2-}$, $HCO_3^-$, and $F^-$ did not disturb phosphate adsorption, even when their concentrations matched those of phosphate ions in real water experimental samples. The adsorbent was still capable of completely removing phosphorus under these conditions (Figure 5a). To further evaluate practical applicability, a fixed continuous-flow column experiment was conducted using water from the Yuhangtang River, which contained competitive anions and natural organic matter (Table S3). The influent phosphate concentration was 0.20–0.25 mg P/L and the fixed column design is illustrated in Figure S4.

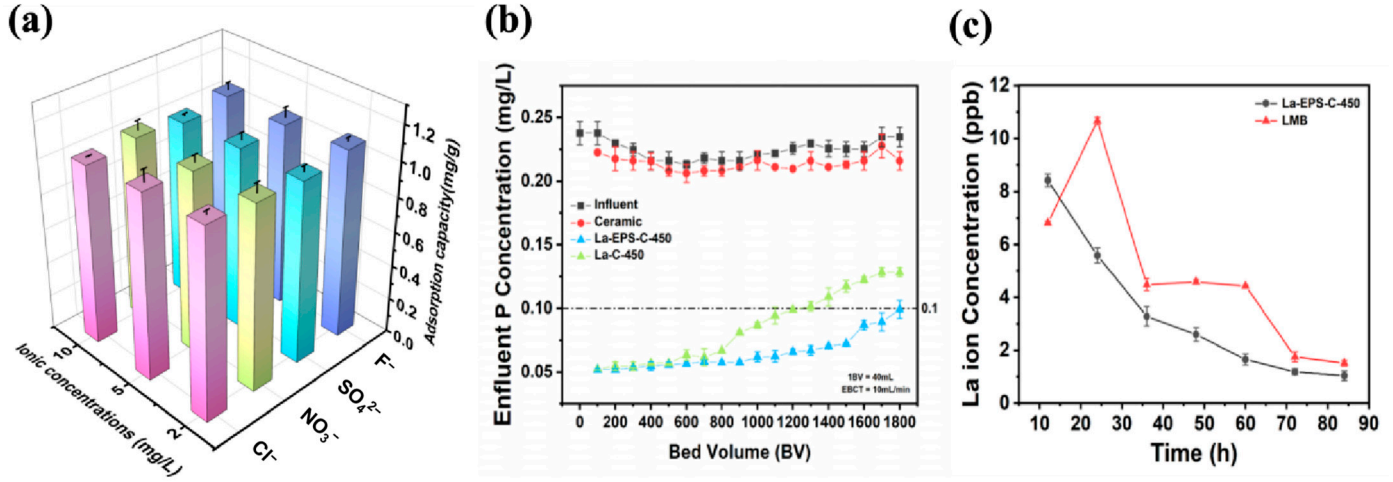



**Figure 5.** The practical application tests. Effects of interfering ions on the adsorption capacity of La-EPS-C-450 (**a**), the performance of phosphorus removal by fixed-bed column (**b**), and the $La^{3+}$ leakage from La-EPS-C-450 and LMB during the treatment of surface water from Qingshan Lake (**c**).

**Table 2.** Phosphorus adsorption capacity of other modified adsorbents.

| Adsorption Material | Adsorption Capacity (mg P/g) | Fitted Adsorption Isotherm | Reference |
|---|---|---|---|
| La-Z | 17.20 | Langmuir | [26] |
| La0.5-PC | 32.40 | Langmuir | [28] |
| ACF-LaOH | 15.30 | Langmuir | [31] |
| LMB | 10.19 | Langmuir | [39] |
| SBP-La | 46.50 | Langmuir | [40] |
| GNS-LaOH | 41.96 | Langmuir | [41] |
| KLa | 24.42 | Langmuir–Freundlich | [42] |
| La-doped silica spheres | 47.89 | Freundlich | [43] |
| DSCT | 14.20 | Langmuir | [44] |

The results indicate that La-EPS-C-450 significantly outperformed commercial ceramic fillers in phosphorus removal. Taking 0.1 mg/L effluent total phosphorus as a treatment target, about 1800 bed volume water was treated by La-EPS-C-450, which is higher than that of La-C-450 (about 1200 bed volume) (Figure 5b). Moreover, in a comparative study using slightly polluted water from Qingshan Lake (initial phosphate concentration = 0.65 mg/L), La-EPS-C-450 and the commercial phosphorus-locking agent LMB were tested for continuous phosphorus removal under similar conditions (Figure S5). While both materials successfully removed phosphorus in the short term, LMB exhibited more pronounced lanthanum ion leakage. In contrast, La-EPS-C-450 exhibited superior lanthanum immobilization, ensuring stable phosphorus binding even as phosphate concentrations increased

(Figure 5c). The experimental results show that the excellent stability of La-EPS-C-450 makes the leaching of lanthanum ion lighter. This feature is particularly important for maintaining the safety of aquatic ecosystems, which can minimize potential metal pollution in water bodies. Compared with other lanthanum-containing biochar materials, these findings highlight the potential of La-EPS-C-450 as an effective and durable adsorbent to remove phosphorus from natural water bodies in practical applications.

## 4. Conclusions

This study highlights the successful development of a lanthanum and extracellular polymeric substance (EPS) coprecipitation-modified ceramic (La-EPS-C-450) for enhanced phosphorus removal. Using commonly available water treatment ceramic fillers as the base matrix, the modified material achieved a maximum phosphorus adsorption capacity of 83.51 mg P/g-La at 25 °C. La-EPS-C-450 demonstrated excellent performance in deep phosphorus removal under both controlled laboratory conditions and real-world applications involving actual river water. The Freundlich model can better describe the adsorption process, indicating multilayer adsorption with a synergistic combination of physical and chemical mechanisms. Chemical adsorption was principally driven by the complexation of hydroxyl groups with phosphate, while electrostatic attraction and ligand exchange between lanthanum and phosphate played significant roles. The material maintained stable adsorption efficiency across a wide pH range of 3–7. La-EPS-C-450 exhibited high selectivity in the presence of competitive anions. Overall, La-EPS-C-450 presents a robust and efficient adsorbent for phosphorus removal, offering significant potential for practical applications in water treatment.

**Supplementary Materials:** The following supporting information can be downloaded at https://www.mdpi.com/article/10.3390/w17081237/s1. Figure S1: Adsorption kinetics of adsorbent precursor before loading onto ceramic; Figure S2: Zeta potential of La-EPS-C-450; Figure S3: Three-dimensional excitation emission matrix spectra (3D-EEM) of activated sludge EPS; Figure S4: Up-flow continuous device; Figure S5: La-EPS-C-450 (left) and LMB (right) short-term phosphorus removal reaction device; Figure S6: The cyclic stability of La-EPS-450 composite adsorption phosphorus removal. Experimental conditions: initial phosphorus concentration 20mg/L. The adsorbent dosage was 5g, the temperature was 25 °C, the initial pH = 7; Table S1: Basic property of La-EPS-C-450; Table S2: Adsorption kinetics parameters of different adsorbents; Table S3: Coexisting anions concentration in influent.

**Author Contributions:** Y.-Y.L.: Conceptualization, methodology, investigation, and original draft preparation. C.-X.Y.: Visualization, resources, investigation. K.-Y.C.: Methodology, validation. J.-J.W.: Conceptualization, resources, writing—reviewing and editing. B.-C.H.: Supervision, conceptualization, funding acquisition, writing—reviewing and editing. R.-C.J.: Writing—reviewing and editing. All authors have read and agreed to the published version of the manuscript.

**Funding:** This work was supported by the "Pioneer" and "Leading Goose" R&D Program of Zhejiang (2023C03149).

**Data Availability Statement:** The datasets generated and analyzed during the current study are available from the corresponding author upon reasonable request.

**Conflicts of Interest:** The authors declare that they have no known competing financial interests or personal relationships that could have appeared to influence the work reported in this paper.

## References

1. Gruau, G.; Legeas, M.; Riou, C.; Gallacier, E.; Martineau, F.; Hénin, O. The oxygen isotope composition of dissolved anthropogenic phosphates: A new tool for eutrophication research? *Water Res.* **2004**, *39*, 232–238. [CrossRef] [PubMed]

2. Schindler, D.W.; Carpenter, S.R.; Chapra, S.C.; Hecky, R.E.; Orihel, D.M. Reducing phosphorus to curb lake eutrophication is a success. *Environ. Sci. Technol.* **2016**, *50*, 8923–8929. [CrossRef] [PubMed]
3. Du, M.; Zhang, Y.; Wang, Z.; Lv, M.; Tang, A.; Yu, Y.; Qu, X.; Chen, Z.; Wen, Q.; Li, A. Insight into the synthesis and adsorption mechanism of adsorbents for efficient phosphate removal: Exploration from synthesis to modification. *Chem. Eng. J.* **2022**, *442*, 136147. [CrossRef]
4. Loganathan, P.; Vigneswaran, S.; Kandasamy, J.; Bolan, N.S. Removal and recovery of phosphate from water using sorption. *Crit. Rev. Environ. Sci. Technol.* **2014**, *44*, 741311. [CrossRef]
5. Liu, B.; Gai, S.; Lan, Y.; Cheng, K.; Yang, F. Metal-based adsorbents for water eutrophication remediation: A review of performances and mechanisms. *Environ. Res.* **2022**, *212*, 113353. [CrossRef] [PubMed]
6. Wu, J.; Zhong, Y.; Hao, C.; Chen, J.; Gao, H.; Han, S.; Shen, Y.; Wang, X. Emulsion synthesis of cellulose/lanthanum alginate /La(III) composite microspheres for efficient and selective adsorption of phosphate. *Chem. Eng. J.* **2024**, *488*, 150949. [CrossRef]
7. Wang, Z.H.; Xia, D.W.; Cui, S.J.; Yu, W.P.; Wang, B.T.; Liu, H.Z. A high-capacity nanocellulose aerogel uniformly immobilized with a high loading of nano-La(OH)$_3$ for phosphate removal. *Chem. Eng. J.* **2022**, *433*, 134439. [CrossRef]
8. Tang, Q.; Shi, C.H.; Shi, W.M.; Huang, X.L.; Ye, Y.Y.; Jiang, W.; Kang, J.X.; Liu, D.Q.; Ren, Y.Z.; Li, D.S. Preferable phosphate removal by nano-La(III) hydroxides modified mesoporous rice husk biochars: Role of the host pore structure and point of zero charge. *Sci. Total Environ.* **2019**, *662*, 511–520. [CrossRef]
9. Zhang, Y.; Ahmed, S.; Zheng, Z.; Liu, F.; Leung, C.-F.; Choy, T.-Y.; Kwok, Y.-T.; Pan, B.; Lo, I.M.C. Validation of pilot-scale phosphate polishing removal from surface water by lanthanum-based polymeric nanocomposite. *Chem. Eng. J.* **2021**, *412*, 128630. [CrossRef]
10. Li, G.; Zhu, W.; Zhong, J.; Sun, J.; Wang, Y.; Mu, B.; Wang, X.; Xu, Y. Efficient phosphate recovery and treatment of high-phosphorus wastewater using sodium alginate-immobilized microspheres based on aluminum-rich water treatment plant sludge. *Environ. Pollut.* **2024**, *363*, 125139. [CrossRef]
11. Wang, C.; Shan, S.; Yang, Z.; Xu, X.; Huang, X.; Li, X.; Liu, S.; Li, B.; Xu, Y.; Li, D. Synchronous sequestration of inorganic and organic phosphorus from eutrophic surface water and sediments via recoverable La-CaO2@HNTs/SA hydrogel beads. *Chem. Eng. J.* **2024**, *499*, 156593. [CrossRef]
12. Feng, C.; Pan, X.; Lin, X.; Yang, Y.; Fan, F.; Jiang, C.; Mei, Y. Capacitive deionization exploiting La-based LDH composite electrode toward energy efficient and selective removal of phosphate. *Desalination* **2024**, *594*, 118259. [CrossRef]
13. Fu, C.; Li, Y.; Zuo, Y.; Li, B.; Liu, C.; Liu, D.; Fu, Y.; Yin, Y. Fabrication of lanthanum/chitosan co-modified bentonite and phosphorus removal mechanism from low-concentration landscape water. *Water Sci. Technol.* **2022**, *86*, 1017–1033. [CrossRef] [PubMed]
14. Kong, H.; Li, Q.; Zheng, X.; Chen, P.; Zhang, G.; Huang, Z. Lanthanum modified chitosan-attapulgite composite for phosphate removal from water: Performance, mechanisms and applicability. *Int. J. Biol. Macromol.* **2023**, *224*, 984–997. [CrossRef] [PubMed]
15. Banik, C.; Lawrinenko, M.; Bakshi, S.; Laird, D.A. Impact of pyrolysis temperature and feedstock on surface charge and functional group chemistry of biochars. *J. Environ. Qual.* **2018**, *47*, 452–461. [CrossRef]
16. Lian, J.; Yang, Y.; Qiu, W.; Huang, L.; Wang, C.; Chen, Q.; Ke, Q.; Wang, Q. Fluorescent characteristics and metal binding properties of different molecular weight fractions in stratified extracellular polymeric substances of activated sludge. *Separations* **2021**, *8*, 120. [CrossRef]
17. Yan, P.; Xia, J.-S.; Chen, Y.-P.; Liu, Z.-P.; Guo, J.-S.; Shen, Y.; Zhang, C.-C.; Wang, J. Thermodynamics of binding interactions between extracellular polymeric substances and heavy metals by isothermal titration microcalorimetry. *Bioresour. Technol.* **2017**, *232*, 354–363. [CrossRef]
18. Peng, S.; Hu, A.; Ai, J.; Zhang, W.; Wang, D. Changes in molecular structure of extracellular polymeric substances (EPS) with temperature in relation to sludge macro-physical properties. *Water Res.* **2021**, *201*, 117316. [CrossRef]
19. Ghodake, G.S.; Shinde, S.K.; Kadam, A.A.; Saratale, R.G.; Saratale, G.D.; Kumar, M.; Palem, R.R.; Al-Shwaiman, H.A.; Elgorban, A.M.; Syed, A.; et al. Review on biomass feedstocks, pyrolysis mechanism and physicochemical properties of biochar: State-of-the-art framework to speed up vision of circular bioeconomy. *J. Clean. Prod.* **2021**, *297*, 126645. [CrossRef]
20. Liu, X.; Liu, J.; Deng, D.; Li, R.; Guo, C.; Ma, J.; Chen, M. Investigation of extracellular polymeric substances (EPS) in four types of sludge: Factors influencing EPS properties and sludge granulation. *J. Water Process. Eng.* **2021**, *40*, 101924. [CrossRef]
21. Al-Ghouti, M.A.; Da'ana, D.A. Guidelines for the use and interpretation of adsorption isotherm models: A review. *J. Hazard. Mater.* **2020**, *393*, 122383. [CrossRef] [PubMed]
22. Krishna Veni, D.; Kannan, P.; Jebakumar Immanuel Edison, T.N.; Senthilkumar, A. Biochar from green waste for phosphate removal with subsequent disposal. *Waste Manag.* **2017**, *68*, 752–759. [CrossRef] [PubMed]
23. Lu, Y.; Wang, H.; Lu, Y.-Y.; Ren, Z.-Q.; Gao, N.; Wang, J.-J.; Huang, B.-C.; Jin, R.-C. In-situ synthesis of lanthanum-coated sludge biochar for advanced phosphorus adsorption. *J. Environ. Manag.* **2024**, *373*, 13607. [CrossRef]
24. Pan, B.; Han, F.; Nie, G.; Wu, B.; He, K.; Lu, L. New strategy to enhance phosphate removal from water by hydrous manganese oxide. *Environ. Sci. Technol.* **2014**, *48*, 5101–5107. [CrossRef]

25. Fu, H.; Yang, Y.; Zhu, R.; Liu, J.; Usman, M.; Chen, Q.; He, H. Superior adsorption of phosphate by ferrihydrite-coated and lanthanum-decorated magnetite. *J. Colloid Interf. Sci.* **2018**, *530*, 704–713. [CrossRef] [PubMed]
26. He, Y.; Lin, H.; Dong, Y.; Wang, L. Preferable adsorption of phosphate using lanthanum-incorporated porous zeolite: Characteristics and mechanism. *Appl. Surf. Sci.* **2017**, *426*, 995–1004. [CrossRef]
27. Liu, M.; Wang, C.; Guo, J.; Zhang, L. Removal of phosphate from wastewater by lanthanum modified bio-ceramisite. *J. Environ. Chem. Eng.* **2021**, *9*, 106123. [CrossRef]
28. Koilraj, P.; Sasaki, K. Selective removal of phosphate using La-porous carbon composites from aqueous solutions: Batch and column studies. *Chem. Eng. J.* **2017**, *317*, 1059–1086. [CrossRef]
29. Wu, B.; Fang, L.; Fortner, J.D.; Guan, X.; Lo, I.M.C. Highly efficient and selective phosphate removal from wastewater by magnetically recoverable $La(OH)_3/Fe_3O_4$ nanocomposites. *Water Res.* **2017**, *126*, 179–188. [CrossRef]
30. Xia, S.; Liang, S.; Qin, Y.; Chen, W.; Xue, B.; Zhang, B.; Xu, G. Significant improvement of adsorption for phosphate removal by lanthanum-loaded biochar. *ACS Omega* **2023**, *8*, 24853–24864. [CrossRef]
31. Zhang, L.; Zhou, Q.; Liu, J.; Chang, N.; Wan, L.; Chen, J. Phosphate adsorption on lanthanum hydroxide-doped activated carbon fiber. *Chem. Eng. J.* **2012**, *185–186*, 160–167. [CrossRef]
32. Lan, Y.; Gai, S.; Cheng, K.; Li, J.; Yang, F. Lanthanum carbonate hydroxide/magnetite nanoparticles functionalized porous biochar for phosphate adsorption and recovery: Advanced capacity and mechanisms study. *Environ. Res.* **2022**, *214*, 113783. [CrossRef]
33. Wei, Y.; Yuan, P.; Zhou, J.; Liu, J.; Losic, D.; Wu, H.; Bu, H.; Tan, X.; Li, Z. Direct atomic-scale insight into the precipitation formation at the lanthanum hydroxide nanoparticle/solution interface. *J. Phys. Chem. Lett.* **2023**, *14*, 3995–4003. [CrossRef] [PubMed]
34. Qiu, H.; Liang, C.; Yu, J.; Zhang, Q.; Song, M.; Chen, F. Preferable phosphate sequestration by nano-La(III) (hydr)oxides modified wheat straw with excellent properties in regeneration. *Chem. Eng. J.* **2017**, *315*, 345–354. [CrossRef]
35. Zhang, Q.; Teng, J.; Zou, G.; Peng, Q.; Du, Q.; Jiao, T.; Xiang, J. Efficient phosphate sequestration for water purification by unique sandwich-like MXene/magnetic iron oxide nanocomposites. *Nanoscale* **2016**, *8*, 7085–7093. [CrossRef]
36. Qu, J.; Akindolie, M.S.; Feng, Y.; Jiang, Z.; Zhang, G.; Jiang, Q.; Deng, F.; Cao, B.; Zhang, Y. One-pot hydrothermal synthesis of $NaLa(CO_3)_2$ decorated magnetic biochar for efficient phosphate removal from water: Kinetics, isotherms, thermodynamics, mechanisms and reusability exploration. *Chem. Eng. J.* **2020**, *394*, 124915. [CrossRef]
37. Pap, S.; Zhao, Q.; Cakin, I.; Gaffney, P.P.J.; Gibb, S.W.; Taggart, M.A. Lanthanum and cerium functionalised forestry waste biochar for phosphate removal: Mechanisms and real-world applications. *Chem. Eng. J.* **2024**, *494*, 152848. [CrossRef]
38. Yu, J.; Xiang, C.; Zhang, G.; Wang, H.; Ji, Q.; Qu, J. Activation of Lattice Oxygen in LaFe(Oxy)hydroxides for Efficient Phosphorus Removal. *Environ. Sci. Technol.* **2019**, *53*, 9073–9080. [CrossRef]
39. Haghseresht, F.; Wang, S.; Do, D.D. A novel lanthanum-modified bentonite, Phoslock, for phosphate removal from wastewaters. *Appl. Clay Sci.* **2009**, *46*, 369–375. [CrossRef]
40. Pan, J.; Yang, H.; Liu, L.; Li, B.; Tang, X.; Wu, X.; Zhang, L.; Ying, G.-G. Sludge-based biochar with lanthanum modification for phosphate recovery from wastewater streams. *Environ. Sci-Wat. Res.* **2022**, *8*, 2873–2883. [CrossRef]
41. Zhang, L.; Gao, Y.; Zhou, Q.; Kan, J.; Wang, Y. High-performance removal of phosphate from water by graphene nanosheets supported lanthanum hydroxide nanoparticles. *Water Air Soil Pollut.* **2014**, *225*, 1967. [CrossRef]
42. Li, J.-R.; Wang, F.-K.; Xiao, H.; Xu, L.; Fu, M.-L. Layered chalcogenide modified by Lanthanum, calcium and magnesium for the removal of phosphate from water. *Colloid Surface A* **2018**, *560*, 306–314. [CrossRef]
43. Huang, W.; Zhu, Y.; Tang, J. Lanthanum-doped ordered mesoporous hollow silica spheres as novel adsorbents for efficient phosphate removal. *J. Mater. Chem. A* **2014**, *2*, 8839–8848. [CrossRef]
44. Yao, Y.; Gao, B.; Inyang, M.; Zimmerman, A.R.; Cao, X.; Pullammanappallil, P.; Yang, L. Removal of phosphate from aqueous solution by biochar derived from anaerobically digested sugar beet tailings. *J. Hazard. Mater.* **2011**, *190*, 501–507. [CrossRef]


**Disclaimer/Publisher's Note:** The statements, opinions and data contained in all publications are solely those of the individual author(s) and contributor(s) and not of MDPI and/or the editor(s). MDPI and/or the editor(s) disclaim responsibility for any injury to people or property resulting from any ideas, methods, instructions or products referred to in the content.